Progress In Electromagnetics Research C, Vol. 34, 239–251, 2013

BEHAVIORAL MODELING OF RF POWER AMPLIFIERS WITH MEMORY EFFECTS USING ORTHONORMAL HERMITE POLYNOMIAL BASIS NEURAL NETWORK

X.-H. Yuan and Q.-Y. Feng*

School of Information Science and Technology, Southwest Jiaotong University, Chengdu, Sichuan 610031, China

Abstract—Behavioral modeling technique provides an efficient and convenient way to analyze and predict the performance of the RF power amplifiers (PAs) in system-level, and thus helps to construct a suitable predistorter to linearize the PA system. To accurately describe the nonlinear dynamic characteristics of PAs, an orthonormal Hermite polynomial basis neural network (OHPBNN) is utilized to represent the PA behavioral model, which outperforms, mainly in respect of modeling accuracy, the classic feedforward neural network using sigmoid activation functions. In addition, we apply an adaptive algorithm to determine the appropriate memory depth of PA behavioral model. Simulation results show that the proposed model provides more accurate prediction of the PAs output signal compared with classic neural network models.

1. INTRODUCTION

The RF power amplifiers (PAs) are essential components in modern wideband wireless communication systems, the purpose of which is to boost the radio signal to sufficient power level for transmission through the air interface from the transmitter to the receiver. However, PAs are inherently nonlinear components, especially when operating close to saturation for power efficiency considerations [1–5], which induces in-band and out-of-band distortions and thus degrades the communication performance. Behavioral modeling is crucial to predict the nonlinearity of PAs in system analysis and estimation, and it is also a key step in constructing a suitable linearizer for the communication system.

Received 19 September 2012, Accepted 15 November 2012, Scheduled 21 November 2012
* Corresponding author: Quanyuan Feng (fengquanyuan@163.com).

Recently, PA behavioral models have attracted much interest as a means of characterizing PAs. The key advantage of behavioral modeling lies in the fact that it does not require deep knowledge of the RF circuit physics and functionality, but simplifies the modeling of the RF circuit to the identification of a mathematical formulation that relates the input and the output of the device under test (DUT) that can be considered as a black box. Consequently, behavioral modeling appears as a time- and resource-efficient process for transmitter performance evaluation and digital predistorter design.

In general, PA behavioral models can be classed into memoryless behavioral models and behavioral models with memory effects. Different memoryless PA models have been proposed in the past, such as the Saleh model [6], the memoryless polynomial model [7], the lookup table (LUT) model [8], etc.. The memoryless behavioral models are simple, efficient and effective for PAs applied in narrowband systems. However, with the increase in the signal bandwidth, the memory effects of PAs can no longer be ignored since it has a more and more significant influence on the system's nonlinear distortion. Thus behavioral modeling of PAs with memory effects is the research focus of many authors in the recent years and various model topologies have been proposed. Volterra series is a general nonlinear model with memory and has been used to model PAs with mild nonlinearities [9–11], however, its prohibitive complexity and restricted applicability to mildly nonlinear PAs have limited the applications of the Volterra model. To avoid the disadvantages of the Volterra model, various modified Volterra models have been proposed. A special case of the Volterra model is the memory polynomial model proposed by Kim et al. [2]. The memory polynomial model [12–14] is currently the most popular derivation of the Volterra model that abandoned the cross terms to alleviate the complexity. Nevertheless, the identification process of the parameters of the memory polynomial model is still relatively computationally complex and perhaps suffers from instability. Alternatively, two-box models, generally known as Wiener or Hammerstein models [15, 16], which are the cascade of a linear block and a static nonlinearity, have been proposed to model the dynamic nonlinearity of PAs. In the two-box, the memoryless nonlinearity is, in most cases, described by a polynomial, while a finite impulse response (FIR) filter is selected to form the linear block due to its good stability. But these models do not consider the nonlinear behavioral of the memory effects and cross terms, which limits the modeling performance. What more, the parameter identification process for both the linear dynamic and static nonlinear blocks has to be carried out separately.

Over the last decade, artificial neural networks (ANNs) have emerged as an efficient and powerful computational tool and have been widely used in in pattern recognition, signal processing, system identification, and control. The neural network approach has also been investigated as one of the modeling and predistortion techniques for PAs because of its adaptive nature and the claim of a universal approximation capability. Different neural topologies and computation algorithms have been proposed [17–22]. Now the ANN-based models are seen as a potential alternative to model RF PAs having medium-to-strong memory effects along with high-order nonlinearity.

However, it should be noted that, although the neural networks have been successfully used in the fields of PA behavioral modeling and predistortion, they suffer from some significant issues, such as the model accuracy, the efficient algorithms and the architecture of the neural network. In this paper, an orthonormal Hermite polynomial basis neural network (OHPBNN) is utilized to represent PA behavioral model, which outperforms, mainly in respect of approximation performance, the most frequently used feedforward neural network using sigmoid activation functions. In addition, we apply an adaptive algorithm to determine the appropriate time delay taps of the PA behavioral model.

2. OHPBNN PA BEHAVIORAL MODEL

2.1. Comparative Analysis of ANN-based PA Behavioral Models

During the past decade, artificial neural network technology has been successfully applied to RF and microwave applications since it can approximate any real function of interest to any desired degree

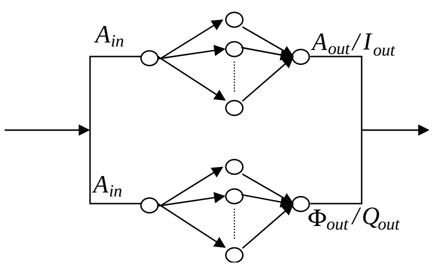

Figure 1. Two separate and uncoupled real-valued neural networks.

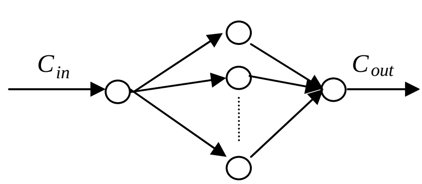

Figure 2. complex-value-based neural network.

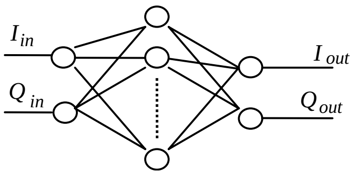

Figure 3. RVFFNN neural network.

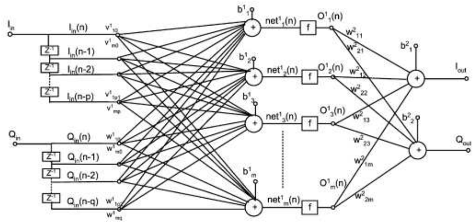

Figure 4. RVFTDNN neural network.

of accuracy due to its universal approximation capability. Various topologies of ANNs were reported in the literature for PAs behavioral modeling [17–22]. In [17], two separate and uncoupled real-valued neural networks were used to model the output amplitude and phase (or the output I and Q components) with the input signal amplitude as the two neural networks' input, as shown in Figure 1. Although this topology is simple and computational efficient, it may suffer from the problem of convergence since the two neural networks are trained separately. Alternatively, [21] proposed to apply a complex-value neural network to the complex signal directly, as shown in Figure 2. In this case, both the weights and activation functions of the network are complex. This type of ANN has to undergo a cumbersome complex training algorithm, increasing the computational burden. To avoid the disadvantages mentioned above, a more effective approach, called the real-valued feedforward neural network (RVFFNN) [22], is proposed as shown in Figure 3. the RVFFNN model takes advantage of simple implementation and low computational complex. Although this topology has been found effective for behavioral modeling of dynamic nonlinear PAs, it falls short of expectations when the PA shows strong memory effects. Considering the memory effects of the PA, the baseband output I_{out} and Q_{out} components of the PA at instant n are a function of p past value of the baseband input I_{in} and q values of the baseband input Q_{in} according to (1) and (2) as follows:

$$I_{out}(n) = f_I \left[I_{in}(n), I_{in}(n-1), \ldots, I_{in}(n-p), Q_{in}(n), Q_{in}(n-1), \ldots, Q_{in}(n-q)\right] \quad (1)$$

$$Q_{out}(n) = f_Q \left[I_{in}(n), I_{in}(n-1), \ldots, I_{in}(n-p), Q_{in}(n), Q_{in}(n-1), \ldots, Q_{in}(n-q)\right] \quad (2)$$

Based on Equations (1) and (2), Liu et al. [18] proposed a new neural network topology, as shown in Figure 4, called the real-valued focus time-delay neural network (RVFTDNN) to account for the memory effects, which was found effective in modeling PAs with memory effects.

2.2. OHPBNN PA Behavioral Model

In this paper, we apply the orthonormal Hermite polynomial basis neural network (OHPBNN) to construct the dynamic nonlinear behavioral model of PA. The OHPBNN model utilizes the same topology as the RVFTDNN model but adopts the orthonormal Hermite polynomial basis functions as the hidden layer's activation functions. In RVFTDNN, the most commonly used activation function, i.e., the sigmoid function, was used in the hidden layer, which is defined as:

$$f(u) = \frac{1}{(1 + e^{-u})} \tag{3}$$

In place of the sigmoid function, here we propose to use a set of orthonormal Hermite polynomial basis functions, taking advantage of their excellent approximation performance, as the activation functions in the hidden layer with the aim of attaining better performance in terms of accuracy and convergence [23, 24]. The orthogonal Hermite polynomials are defined as follows:

$$\begin{cases} H_0(x) = 1 \\ H_1(x) = 2x \\ H_n(x) = 2xH_{n-1}(x) - 2(n-1)H_{n-2}(x) \end{cases} \tag{4}$$

where $H_i(x)$, $i = 0, 1, 2, \ldots$, is the ith-order term of the orthogonal Hermite polynomial. It should be noted that the terms are orthogonal with each other and there is a recursive relationship between the terms, which helps to alleviate the computational burden. Based on the representations given above, the orthonormal Hermite polynomials are defined as:

$$h_n(x) = a_n H_n(x) \varphi(x) \quad n = 0, 1, 2, \ldots \tag{5}$$

where

$$a_n = (n!)^{-1/2} \pi^{1/4} 2^{-(n-1)/2} \tag{6}$$

$$\varphi(x) = \left(1/\sqrt{2\pi}\right) e^{-x^2/2}. \tag{7}$$

The orthonormal Hermite terms are also orthogonal and have the property of universal approximation, i.e., they have the capability of approximating any real function of interest to any desired accuracy. In the proposed OHPBNN behavioral model in this paper, the terms $h_n(x)$, $n = 0, 1, 2, \ldots$, are chosen as the activation functions of the hidden neurons of the neural network. The orthonormal Hermite terms are assigned from the lowest order term to the higher order ones in the hidden neurons, as shown in Figure 5. The OHPBNN model

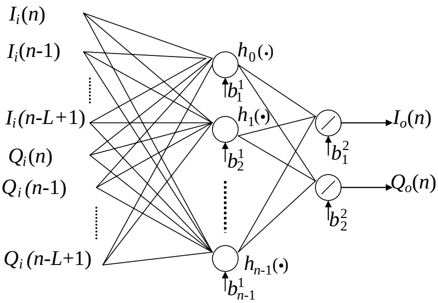

Figure 5. OHPBNN PA behavioral model.

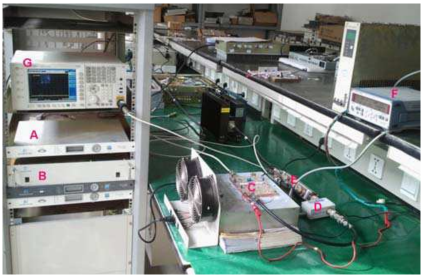

Figure 6. Test platform.

utilizes the baseband signal's in-phase and quadrature components as its inputs and outputs. There are $2L$ inputs, including L inphase components and L quadrature ones, n hidden neurons and 2 outputs representing the PA's current baseband outputs. Here L is considered as the number of time-delay taps of the OHPBNN model. The hidden layer of neural network can be considered as a nonlinear mapping and thus it's just equivalent to an orthonormal Hermite polynomial which has excellent approximation capability. By applying the more complicated and orthogonal basis functions as the hidden layer's activation functions, the OHPBNN is expected to attain more accurate approximation performance, but with less number of hidden neurons, than the classic neuron network with identical sigmoid functions as activation functions.

3. TRAINING ALGORITHM AND VALIDATION RESULTS

For validation of the proposed OHPBNN PA behavioral model, low-pass equivalent input-output data were measured on a class-AB power amplifier with an average output power of 50.4 dBm using MMB (Mobile Multimedia Broadcasting) signal. The signal bandwidth was 7.56-MHz. Figure 6 shows the test platform to obtain measured PA input-output data as well as observe PA output. The test MMB signal, generated by a MMB signal generator (A), was fed to the DUT (power amplifier) (C) after preamplification of a high-gain preamplifier stage (B). The output of the DUT was then, through a power meter probe (D) and a directional coupler (E), sent to the MMB signal generator where PA input and output data were sampled for model extraction and validation. The power spectrum density (PSD) and power level of PA output signal were also presented on the spectrum analyzer (G) and the power meter (F), respectively. The measured data were first synchronized using cross-correlation technique for time alignment and then divided into two sets. One set was used for training purpose and the other for validation.

3.1. Memory Depth Estimation of PA Behavioral Model

When applied with narrowband signals, PA can be considered as a memoryless component. In this case, the neural network for PA behavioral modeling uses only the current input signal as its input. But as for high power PAs fed with wideband signals, the memory effects can no longer be ignored and should be taken into account in the behavioral modeling procedure. Thus it's a preceding and important task to estimate the degree of PA's memory effect which determines the appropriate number of inputs (or time-delay taps) of neural network model. Here we employ an adaptive algorithm to estimate the PA's memory depth. The algorithm updates the OHPBNN network weights by minimizing the mean-squared error (MSE) which is defined as follows:

$$MSE = \frac{1}{2N}\sum_{n=1}^{N}\left[(I_o(n)-\bar{I}_o(n))^2+(Q_o(n)-\bar{Q}_o(n))^2\right] \qquad (8)$$

where I_o and Q_o are the measured outputs, and $\bar{I}_o$ and $\bar{Q}_o$ represent the outputs of the behavioral model. N is the total number of the training samples.

The main ideal of the adaptive algorithm is that, during the training procedure, the neural network model is dynamically constructed through an incremental constructive method. At first, a simplest neural network topology is given, which has only two inputs ($I_i(n)$ and $Q_i(n)$), two outputs and one hidden neuron in the hidden layer. Then the adaptive algorithm trains the network by dynamically increasing the hidden neurons as well as the time-delay taps (i.e., the input neurons). The whole training procedure is as follows:

(1) Set the initial OHPBNN network architecture, which includes: two inputs ($I_i(n)$ and $Q_i(n)$), one hidden neuron with activation function h_o, and two outputs ($I_o(n)$ and $Q_o(n)$).

(2) Train the hidden layer through an incremental constructive method. The hidden neurons are dynamically increased during this step until MSE performance fails to improve. For the hidden layer is equivalent to a functional series expansion utilizing the orthonormal Hermite polynomials and where each additional term

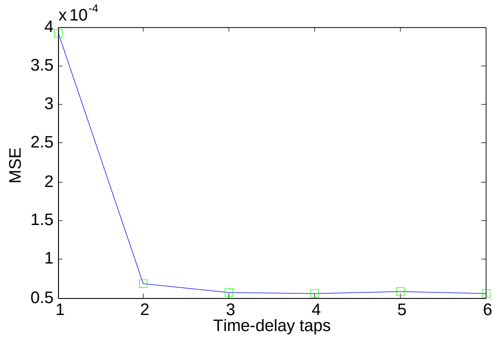

Figure 7. MSE variation versus the number of time-delay taps of OHPBNN PA behavioral model.

in the expansion contributes to improving the accuracy of the approximation, MSE will become smaller as more hidden neurons, having higher order orthonormal Hermite terms, are included.

(3) Increase one time-delay tap in the input layer, i.e., add one previous input to the network, thus the OHPBNN model can account for more memory effects.

(4) The weights attached to the new input neuron are first trained for a fixed iterative times by freezing the existing neurons' weights. Then the algorithm trans the whole network to further minimize MSE error.

(5) If the MSE error decreases enough during step (4), then go to (3) and continue to increase the time-delay taps; or else, execute the following steps.

(6) Further train the hidden layer by appropriately increasing the hidden neurons.

(7) If the MSE error decreases enough during step (6), then go to (3) and continue to increase the time-delay taps; or else, stop the algorithm.

Through the above algorithm, the exact number of time-delay taps required for the behavioral modeling can be found. Figure 7 shows the MSE variation with respect to the number of time-delay taps. It can be seen from the figure that the OHPBNN PA model with 3 time-delay taps approximates the minimum MSE, suggesting the appropriate memory depth in constructing the behavioral model. However, it should be noted that, to reinforce the adaptive algorithm, here we have made some modifications to it so that the MSE performance for much more time-delay taps were inspected and presented in this figure. The optimal number of time-delay taps shown in this figure will be applied in the following section.

3.2. Validation Results

Figure 8 shows the power spectra density for the PA output, the OHPBNN and the RVFTDNN model prediction. As seen form this figure, both the OHPBNN and RVFTDNN model exhibit good in-band modeling performance, but the RVFTDNN model fails to precisely describe the out-of-band PA characteristic. To inspect the in-band modeling performance, the power spectra density of error signals both for the OHPBNN and RVFTDNN model are presented in Figure 9. Results from Figures 8 and 9 show that the OHPBNN model has much better modeling performance, both for in-band and out-of-band regions, than RVFTDNN model. For the time-domain comparison, the NMSE is adopted as a metric and the results are presented in

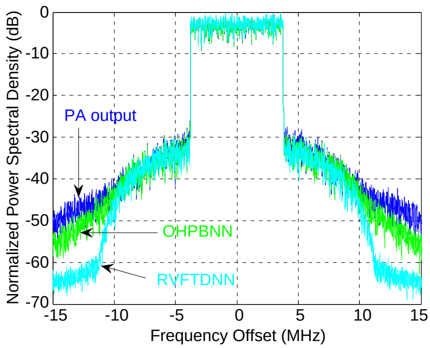

Figure 8. PSD comparison for the PA output, OHPBNN model and RVFTDNN model prediction.

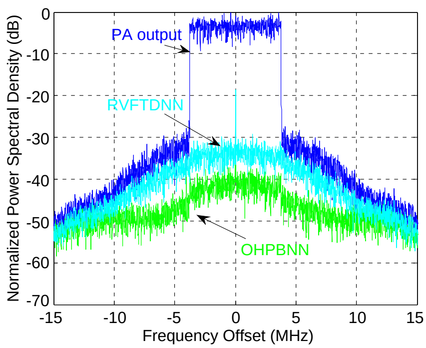

Figure 9. PSD of the error signals both for the OHPBNN and RVFTDNN.

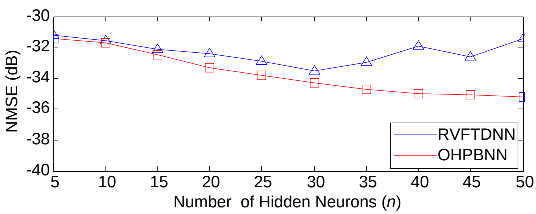

Figure 10. NMSE variation versus the number of hidden neurons both for OHPBNN and RVFTDNN model.

Figure 10. The NMSE for OHPBNN decreases steadily with the increase of hidden neurons. This supports our initial statement in the paper that the OHPBNN will become more accurate as more hidden neurons, having higher order orthonormal Hermite terms, are added to the network. Although the minimum NMSE for RVFTDNN is acquied when there are 30 hidden neurons according to Figure 10, careful inspection is still needed before constructing the best RVFTDNN model to find the optimal number of hidden neurons. In this paper, the number of hidden neurons is 35 both for the RVFTDNN and

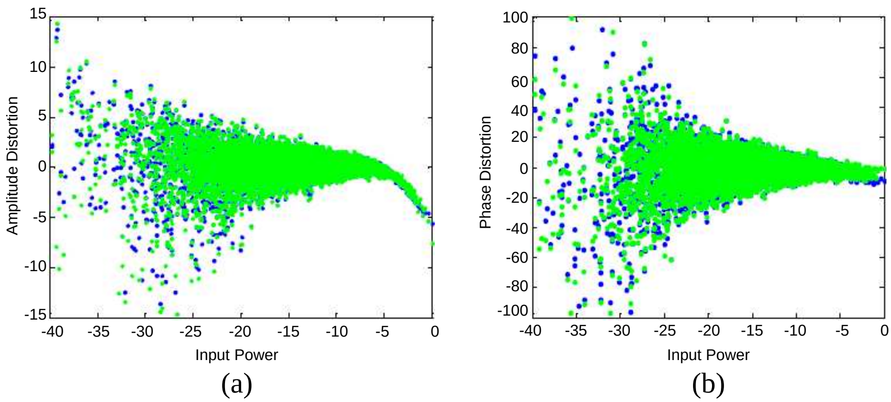

Figure 11. Dynamic nonlinear AM/AM and AM/PM characteristic comparison between the PA output and OHPBNN prediction. (a) AM/AM. (b) AM/PM.

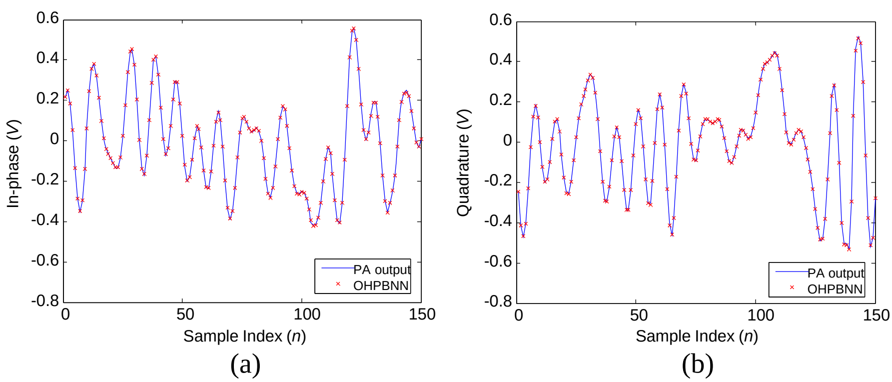

Figure 12. Time-domain validation for OHPBNN model. (a) In-phase component. (b) Quadrature component.

OHPBNN models for comparison purpose. In Figure 11, dynamic nonlinear AM/AM and AM/PM characteristics are shown both for the measured PA output and the OHPBNN prediction. From this figure, it can also be seen that there is a very promising agreement between the measured and OHPBNN prediction in terms of dynamic nonlienar AM/AM and AM/PM conversion characteristics. Note that the AM/AM and AM/PM responses show the hysteresis dependency of the power amplifier on the history of past input signals. Figure 12 presents the in-phase and quadrature channel signal which provides the validation in time domain.

4. CONCLUSION

In this paper, the orthonormal Hermite polynomial basis neural network is utilized for dynamic nonlinear PA behavioral modeling. The OHPBNN PA behavioral model uses orthonormal Hermite basis functions as the hidden layer's activation functions, providing more accurate modeling performance, both for in-band and out-of-band regions, compared with RVFTDNN model. In addition, an adaptive algorithm is also proposed to estimate the memory depth of PA behavioral model. Validation results on a class-AB power amplifier using MMB signals with 7.56 MHz signal bandwidth demonstrates the superior performance of the OHPBNN model.

ACKNOWLEDGMENT

This work is supported by the National Natural Science Foundation of China (NNSF) under Grant 60990320, 60990323, 61271090, the National 863 Project of China under Grant 2012AA012305, Sichuan Provincial Science and technology support Project under Grant 2012GZ0101, and Chengdu Science and technology support Project under Grant 12DXYB347JH-002. The authors would like to express their gratitude to Dr. Liangchen Zhou for his affording the experimental data and valuable discussions on this paper.

REFERENCES

1. Ghannouchi, F. M. and O. Hammi, "Behavioral modeling and predistortion," *IEEE Microwave Mag.*, Vol. 10, No. 7, 52–64, Dec. 2009.
2. Kim, J. and K. Konstantinou, "Digital predistortion of wideband signals based on power amplifier model with memory," *Electron. Lett.*, Vol. 37, No. 23, 1417–1418, Nov. 2001.

3. Thein, T. T., C. L. Law, and K. Fu, "Frequency domain dynamic thermal analysis in GaAs HBT for power amplifier applications," *Progress In Electromagnetics Research*, Vol. 118, 71–87, 2011.
4. Zhang, B., Y.-Z. Xiong, L. Wang, S. Hu, T.-G. Lim, Y.-Q. Zhuang, and J. L.-W. Li, "A D-band power amplifier with 30-GHz bandwidth and 4.5-dBm Psat for high-speed communication system," *Progress In Electromagnetics Research*, Vol. 107, 161–178, 2010.
5. Zhu, A. and T. J. Brazil, "Behavioral modeling of RF power amplifiers based on pruned volterra series," *IEEE Microwave and Wireless Components Lett.*, Vol. 14, 563–565, Dec. 2004.
6. Saleh, A., "Frequency-independent and frequency-dependent nonlinear models of TWT amplifiers," *IEEE Trans. Commun.*, Vol. 29, No. 11, 1715–1720, Nov. 1981.
7. D'Andrea, A. N., V. Lottici, and R. Reggiannini, "RF power amplifier linearization through amplitude and phase predistortion," *IEEE Trans. Commun.*, Vol. 44, No. 11, 1477–1484, Nov. 1996.
8. Cavers, J. K., "A linearizing predistorter with fast adaptation," *Proc. IEEE Vehicular Techn. Conf.*, 41–47, May 1990.
9. Schetzen, M., *The Volterra and Wiener Thoeries Nonlinear Systems*, Wiley, New York, 1980.
10. Zhu, A., M. Wren, and T. J. Brazil, "An efficient Volterra-based behavioral model for wideband RF power amplifiers," *IEEE MTT-S Int. Microwave Symp. Dig.*, Vol. 2, 787–790, Jun. 2003.
11. Zhu, A. and T. J. Brazil, "Behavioral modeling of RF power amplifiers based on pruned Volterra series," *IEEE Microwave and Wireless Components Lett.*, Vol. 14, No. 12, Dec. 2004.
12. Morgan, D. R., Z. Ma, J. Kim, M. G. Zierdt, and J. Pastalan, "A generalized memory polynomial model for digital predistortion of RF power amplifiers," *IEEE Trans. Signal Process.*, Vol. 54, No. 10, 3852–3860, Oct. 2006.
13. Wang, H., J. Bao, and Z. Wu, "Comparison of the behavioral modelings for RF power amplifier with memory effects," *IEEE Microwave and Wireless Components Lett.*, Vol. 19, No. 3, 179–181, Mar. 2009.
14. Ding, L. and G. T. Zhou, "Effects of even-order nonlinear terms on power amplifiers modeling and predistortion linearization," *IEEE Trans. Vehicular Tech.*, Vol. 53, 156–162, Jan. 2004.
15. Liu, T., S. Boumaiza, and F. M. Ghannouchi, "Augmented Hammerstein predistorter for linearization of broad-band wireless

transmitters," *IEEE Trans. Microwave Theory Tech.*, Vol. 54, No. 4, Apr. 2006.

16. Sano, A. and L. Sun, "Identification of Harmmerstein-Wiener system with application to compensation for nonlinear distortion," *Proc. 41st SICE Annu. Conf.*, Vol. 3, 1521–1526, Aug. 2002.
17. Ibnkahla, M., J. Sombrin, F. Castanie, and N. J. Bershad, "Neural networks for modeling nonlinear memoryless communication channels," *IEEE Trans. Commun.*, Vol. 45, 768–771, Jul. 1997.
18. Liu, T., S. Boumaiza, and F. M. Ghannouchi, "Dynamic behavioral modeling of 3G power amplifiers using real-valued time-delay neural networks," *IEEE Trans. Microwave Theory Tech.*, Vol. 52, No. 3, Mar. 2004.
19. Mkadem, F. and S. Boumaiza, "Extended Hammerstein behavioral model using artificial neural networks," *IEEE Trans. Microwave Theory Tech.*, Vol. 57, No. 4, Apr. 2009.
20. Cao, Y., X. Chen, and G. Wang, "Dynamic behavioral modeling of nonlinear microwave devices using real-time recurrent neural network," *IEEE Trans. Electron Devices*, Vol. 56, No. 5, May 2009.
21. Li, M., J. Liu, Y. Jiang, and W. Feng, "Complex-Chebyshev functional link neural network behavioral model for broadband wireless power amplifiers," *IEEE Trans. Microwave Theory Tech.*, Vol. 60, No. 6, Jun. 2012.
22. Naskas, N. and Y. Papananos, "Adaptive baseband predistorter for radio frequency power amplifiers based on a multiplayer perceptron," *9th Int. Electron., Circuits, Syst. Conf.*, Vol. 3, No. 11, 1107–1110, 2002.
23. Lin, F. J., et al., "Tracking control of thrust active magnetic bearing system via hermite polynomial-based recurrent neural network," *IET Electric Power Applications*, Vol. 4, 701–714, 2010.
24. Vrudhula, S., et al., "Hermite polynomial based interconnect analysis in the presence of process variations," *IEEE Transactions on Computer-Aided Design of Integrated circuits and systems*, Vol. 25, 2001–2011, 2006.